Exclusive photoproduction of lepton pairs at LHC

B. Pire [a], L. Szymanowski and J. Wagner [b]

[a] CPHT, École Polytechnique, CNRS, 91128 Palaiseau, France

[b] Soltan Institute for Nuclear Studies, Hoża 69, 00-681 Warsaw, Poland

Exclusive photoproduction of dileptons, $\gamma p \to \ell^+ \ell^- p$, will be measured in ultraperipheral collisions at LHC. The mechanism where the lepton pair comes from a heavy timelike photon radiated from a quark interferes with the pure QED process $\gamma\gamma \to \ell^+\ell^-$. As an analog of deeply virtual Compton scattering, this *timelike Compton scattering* is a way to study generalized parton distributions in the nucleon or the nucleus. High energy kinematics will enable to focus on gluon distributions. Nuclear effects may be scrutinized in heavy ion collisions.

1. Introduction

A considerable amount of theoretical and experimental work has recently been devoted to the study of deeply virtual Compton scattering (DVCS), i.e., $\gamma^* p \to \gamma p$, an exclusive reaction where generalized parton distributions (GPDs) factorize from perturbatively calculable coefficient functions, when the virtuality of the incoming photon is high enough [1]. It is now recognized that the measurement of GPDs should contribute in a decisive way to our understanding of how quarks and gluons assemble themselves to hadrons [2]. In particular the transverse location of quarks and gluons become experimentally measurable via the transverse momentum dependence of the GPDs [3].

The "inverse" process, $\gamma p \to \gamma^* p$ at small t and large *timelike* virtuality Q'^2 of the final state photon, timelike Compton scattering (TCS) [4], shares many features of DVCS. The Bjorken variable in that case is $\tau = Q'^2/s$. The possibility to use high energy hadron colliders as powerful sources of quasi real photons [5] leads to the hope of determining gluonic GPDs in the small skewedness region, which is an essential program complementary to the determination of the quark GPDs at lower energy electron accelerators. Moreover, the crossing from a spacelike to a timelike probe is an important test of the understanding of QCD corrections, as shown by the history of the understanding of the Drell-Yan re-action in terms of QCD.
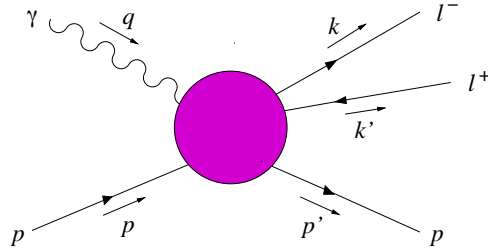

Figure 1. Real photon-proton scattering into a lepton pair and a proton.

The physical process where to observe TCS is photoproduction of a heavy lepton pair, $\gamma p \to \mu^+ \mu^- p$ or $\gamma p \to e^+ e^- p$, shown in Fig. 1. As in the case of DVCS, a Bethe-Heitler (BH) mechanism contributes at the amplitude level. The interference between the TCS and BH processes can readily be accessed through the angular distribution of the lepton pair. In the $\ell^+ \ell^-$ c.m., one introduces the polar and azimuthal angles θ and φ of $\vec{k}$, with reference to a coordinate system with 3-axis along $-\vec{p}'$ and 1- and 2-axes such that $\vec{p}$ lies in the 1-3 plane and has a positive 1-component. This is shown in Fig. 2.
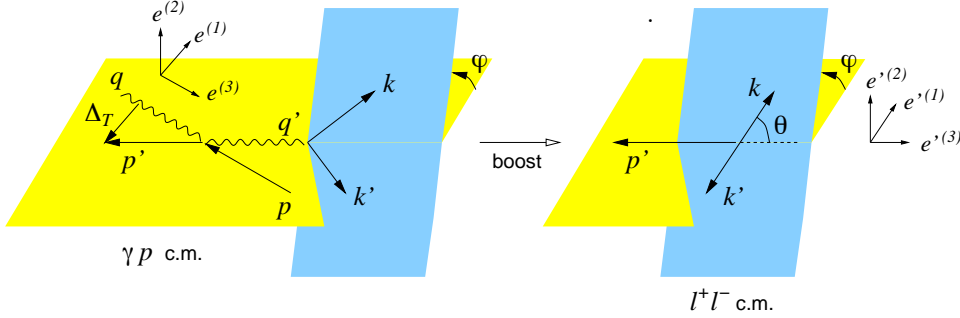
Figure 2. Kinematical variables and coordinate axes in the γp and $\ell^+\ell^-$ c.m. frames.
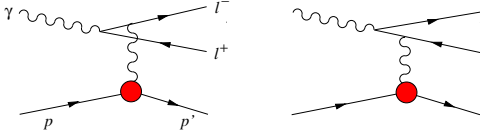

Figure 3. The Feynman diagrams for the Bethe-Heitler amplitude.

2. The various contributions

2.1. The Bethe-Heitler contribution

The Bethe-Heitler amplitude is readily calculated from the two Feynman diagrams in Fig. 3. We parameterize the photon-proton vertex in terms of the usual Dirac and Pauli form factors $F_1(t)$ and $F_2(t)$, normalizing $F_2(0)$ to be the anomalous magnetic moment of the target. Neglecting masses and t compared to terms going with s or Q'^2, the BH contribution to the unpolarized γp cross section is (M is the proton mass)

$$\frac{d\sigma_{BH}}{dQ'^2\,dt\,d(\cos\theta)\,d\varphi} \approx \frac{\alpha_{em}^3}{2\pi s^2}\frac{1}{-t}\frac{1+\cos^2\theta}{\sin^2\theta}$$
$$\left[\left(F_1^2 - \frac{t}{4M^2}F_2^2\right)\frac{2}{\tau^2}\frac{\Delta_T^2}{-t} + (F_1+F_2)^2\right], \quad (1)$$

provided we stay away from the kinematical region where the product of lepton propagators goes

to zero at very small θ. The interesting physics program thus imposes a cut on θ to stay away from the region where the BH cross section becomes extremely large.

2.2. The Compton amplitude

Both DVCS and TCS are limiting cases of the general Compton process

$$\gamma^*(q) + p(p) \to \gamma^*(q') + p(p'), \quad (2)$$

where the four-momenta q and q' of the photons can have any virtuality. Defining $\Delta = p' - p$, the invariants are $Q^2 = -q^2$, $Q'^2 = q'^2$, $s = (p+q)^2$, $t = \Delta^2$ and the scaling variables ξ and η read

$$\xi = -\frac{(q+q')^2}{2(p+p')\cdot(q+q')} \approx \frac{Q^2-Q'^2}{2s+Q^2-Q'^2},$$
$$\eta = -\frac{(q-q')\cdot(q+q')}{(p+p')\cdot(q+q')} \approx \frac{Q^2+Q'^2}{2s+Q^2-Q'^2}, \quad (3)$$

where the approximations hold in the kinematical limit we are working in. x, ξ, and η represent plus-momentum fractions (Light-cone coordinates are defined as $v^\pm = \frac{v^0 \pm v^3}{\sqrt{2}}$, both proton momenta p and p' moving fast to the right, i.e., having large plus-components).

$$x = \frac{(k+k')^+}{(p+p')^+},\ \xi \approx -\frac{(q+q')^+}{(p+p')^+},\ \eta \approx \frac{(p-p')^+}{(p+p')^+}. (4)$$

To leading-twist accuracy one has $\xi = \eta$ in DVCS and $\xi = -\eta$ in TCS.

In the region where at least one of the virtualities is large, the amplitude is given by the convolution of hard scattering coefficients, calculable in perturbation theory, and generalized parton distributions, which describe the nonperturbative physics of the process. To leading order in α_s one then has the quark handbag diagrams of Fig. 4. The analysis of these handbag diagrams show the simple relations

$$M^{\lambda'+,\lambda+}\Big|_{TCS} = \left[M^{\lambda'-,\lambda-}\right]^*_{DVCS},$$

$$M^{\lambda'-,\lambda-}\Big|_{TCS} = \left[M^{\lambda'+,\lambda+}\right]^*_{DVCS} \quad (5)$$

between the helicity amplitudes for TCS and DVCS at equal values of η and t. These relations should be evaluated at corresponding values of Q'^2 and Q^2 since the photon virtualities play analogous roles in providing the hard scale of the respective processes and thus enter in the scale dependence of the parton distributions. The relations (5) tell us that at Born level and to leading twist one obtains the amplitudes for TCS from those of DVCS by changing the sign of the imaginary part and reversing the photon polarizations. To this accuracy, the two processes thus carry exactly the same information on the generalized quark distributions. However, the relations (5) no longer hold at $O(\alpha_s)$, neither for the one-loop corrections to the quark handbag diagrams nor for the diagrams involving gluon distributions. Indeed the TCS amplitude has discontinuities in both s and Q'^2, with one-loop hard scattering diagrams contributing to both cuts. In situations where $O(\alpha_s)$ contributions are important, the DVCS and TCS processes will have a different dependence on the generalized parton distributions.

2.3. The interference term

Since the amplitudes for the Compton and Bethe-Heitler processes transform with opposite signs under reversal of the lepton charge, the interference term between TCS and BH is odd under exchange of the ℓ^+ and ℓ^- momenta, whereas the individual contributions of the two processes are even. Any observable that changes sign under $k \leftrightarrow k'$ will hence project out the interference term, eliminating in particular the eventu-
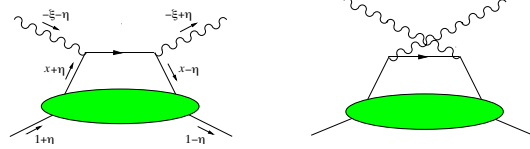

Figure 4. Handbag diagrams for the Compton process (2) in the scaling limit. The plus-momentum fractions x, ξ, η refer to the average proton momentum $\frac{1}{2}(p + p')$.

ally large BH contribution. Clean information on the interference term is therefore contained in the angular distribution of the lepton pair. The interference part of the cross section for $\gamma p \to \ell^+ \ell^- p$ with unpolarized protons and photons is given by

$$\frac{d\sigma_{INT}}{dQ'^2 \, dt \, d(\cos\theta) \, d\varphi} = - \frac{\alpha_{em}^3}{4\pi s^2} \frac{1}{-t} \frac{M}{Q'} \frac{1}{\tau\sqrt{1-\tau}}$$
$$\left[\cos\varphi \frac{1+\cos^2\theta}{\sin\theta}\mathrm{Re}\,\tilde{M}^{--} - \cos 2\varphi \sqrt{2}\cos\theta\,\mathrm{Re}\,\tilde{M}^{0-}\right.$$
$$\left. + \cos 3\varphi \, \sin\theta \, \mathrm{Re}\,\tilde{M}^{+-} + O\!\left(\frac{1}{Q'}\right)\right], \quad (6)$$

with

$$\tilde{M}^{\mu'\mu} = \frac{\Delta_T}{M}\left[(1-\tau)F_1 - \frac{\tau}{2}\,F_2\right]M^{-\mu',-\mu}$$
$$+ \frac{\Delta_T}{M}\left[F_1 + \frac{\tau}{2}\,F_2\right]M^{+\mu',+\mu} - \frac{\Delta_T^2}{2M^2}\,F_2\,M^{+\mu',-\mu}$$
$$+ \left[\tau^2(F_1 + F_2) + \frac{\Delta_T^2}{2M^2}F_2\right]M^{-\mu',+\mu} \quad (7)$$

is the same combination of Compton helicity amplitudes as defined in [6]. The close analogy between TCS and DVCS is manifest, and a γ^* with negative helicity in TCS corresponds to a γ^* with positive helicity in DVCS as already found in the relations (5). Without polarization, one probes the real parts of the Compton helicity amplitudes.

Let us summarize the results of numerical estimates obtained in Ref. [4] in the case of low scattering energy. A model calculation gives the results shown on Fig. 5 for the φ dependence of
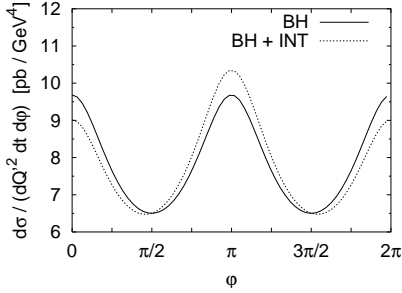
Figure 5.   The cross section integrated over $\theta \in [\pi/4, 3\pi/4]$ as a function of φ for $\sqrt{s} = 5\,\text{GeV}$, $Q'^2 = 5\,\text{GeV}^2$, $|t| = 0.2\,\text{GeV}^2$. The curves represent the BH contribution (solid line) and the sum of BH and the interference term (dash-dotted line).

Figure 6. The ratio R defined in (8). for $\sqrt{s} = 5\,\text{GeV}$ and $Q'^2 = 5\,\text{GeV}^2$. The curves correspond to three models for the GPDs [4].

the cross section integrated over θ in the range $[\pi/4, 3\pi/4]$. With the integration limits symmetric about $\theta = \pi/2$ the interference term is odd under $\varphi \to \pi + \varphi$ due to charge conjugation, whereas the TCS and BH cross sections are even. The contributions from BH and the sum of BH and the interference term are separately shown. The TCS cross section is flat in φ to leading-twist accuracy. In the kinematics of the figure one gets $d\sigma_{TCS}/(dQ'^2\, dt\, d\varphi) \approx 0.2\,\text{pb}\,\text{GeV}^{-4}$ when applying the same cut in θ.

To extract information on the Compton amplitude in a compact way, Ref. [4] demonstrated that it was useful to introduce the ratio R :

$$R = \frac{2 \int_0^{2\pi} d\varphi \, \cos\varphi \, \dfrac{dS}{dQ'^2\, dt\, d\varphi}}{\int_0^{2\pi} d\varphi \, \dfrac{dS}{dQ'^2\, dt\, d\varphi}} \;, \qquad (8)$$

which projects out the ratio a_1/a_0 of Fourier coefficients in the weighted cross section $dS/(dQ'^2\, dt\, d\varphi) = \sum_{n=0}^{\infty} a_n \cos(n\varphi)$. Up to $1/Q'$ suppressed contaminations the numerator in R is proportional to the combination $\tilde{M}^{--}$ of Compton amplitudes, whereas the denominator
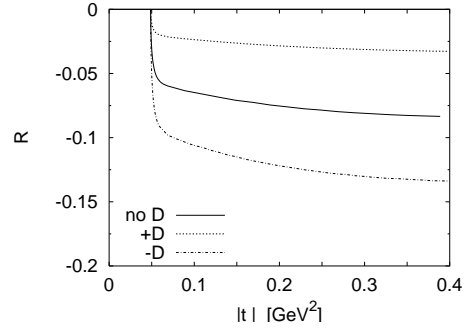
is dominated by the BH part of the cross section. Fig. 6 shows this ratio as a function of t for three models of the GPDs.

Concerning the high energy domain, we are currently working to get an estimate of the different contributions to the lepton pair cross section for ultraperipheral collisions at the LHC. Since the cross sections decrease rapidly with Q'^2, we are interested in the kinematics of moderate Q'^2, say a few GeV^2, and large energy, thus very small values of η. A rough estimate of the Bethe Heitler cross section gives 28 picobarns when it is integrated over θ in the range $[\pi/4, 3\pi/4]$, φ in the range $[0, 2\pi]$, $-t$ in the range $[0.05, 0.25]\text{GeV}^2$ and Q'^2 in the range $[4.5, 5.5]\,\text{GeV}^2$. This gives hope for a measurable process. It remains to check whether one may detect the modulation of this cross section by the interference with the TCS amplitude. The crucial ingredient is realistic models of GPDs at small skewedness. Singlet quark and gluon GPDs will give the dominant contributions to the TCS amplitude in that domain. Since gluon GPDs only enter the TCS amplitude at the $O(\alpha_S)$ level, a consistent treatment requires to take into account GPD evolution equations. This raises the question of the choice of factorization scale in a process where the large scale is timelike, which has been much debated in

the inclusive case of Drell Yan lepton pair production, where enhancement K- factors are usually understood as coming from the analytical continuation of $log(Q'^2)$ terms from spacelike to timelike values. Such factors are likely to be present also in our case.

3. Nuclear targets

The operation of LHC as a heavy ion collider will enable us to study TCS on nuclei. Such scattering may be coherent and one then needs to define nuclear GPDs [7]. This is a very interesting subject which definitely needs more work. Incoherent TCS will also occur on quasi free neutrons and protons. Let us remark that the BH process is suppressed for a neutron target, due to the zero charge of the neutron.

Acknowledgements

REFERENCES

1. D. Müller *et al.*, Fortsch. Phys. **42**, 101 (1994); X. Ji, Phys. Rev. Lett. **78**, 610 (1997); A. V. Radyushkin, Phys. Rev. **D56**, 5524 (1997); J. C. Collins and A. Freund, Phys. Rev. **D59**, 074009 (1999).
2. M. Diehl, Phys. Rept. **388** (2003) 41; A. V. Belitsky and A. V. Radyushkin, Phys. Rept. **418**, 1 (2005); S. Boffi and B. Pasquini, arXiv:0711.2625 [hep-ph].
3. M. Burkardt, Phys. Rev. D **62**, 071503 (2000) and Int. J. Mod. Phys. A **18**, 173 (2003); J. P. Ralston and B. Pire, Phys. Rev. D **66**, 111501 (2002); M. Diehl, Eur. Phys. J. C **25**, 223 (2002).
4. E. R. Berger, M. Diehl and B. Pire, Eur. Phys. J. C **23**, 675 (2002).
5. K. Hencken *et al.*, Phys. Rept. **458**, 1 (2008).
6. M. Diehl *et al.*, Phys. Lett. **B411**, 193 (1997).
7. E. Berger *et al.*, Phys. Rev. Lett. **87**, 142302 (2001); F. Cano and B. Pire, Eur. Phys. J. A **19**, 423 (2004); A. Kirchner and D. Mueller, Eur. Phys. J. C **32**, 347 (2003); V. Guzey and M. Strikman, Phys. Rev. C **68**, 015204 (2003); V. Guzey, arXiv:0801.3235 [nucl-th] and J. Phys. G **32**, 251 (2006).